VCU

Virginia Commonwealth University
VCU Scholars Compass

Electrical and Computer Engineering Publications   Dept. of Electrical and Computer Engineering

2013

Extending device performance in photonic devices using piezoelectric properties

Gregory Edward Triplett
Virginia Commonwealth University, getriplett@vcu.edu

Follow this and additional works at: https://scholarscompass.vcu.edu/egre_pubs

Part of the Electronic Devices and Semiconductor Manufacturing Commons, and the Semiconductor and Optical Materials Commons

PROCEEDINGS OF SPIE

Extending device performance in photonic devices using piezoelectric properties

Gregory E. Triplett

SPIE.

Extending Device Performance in Photonic Devices using Piezoelectric Properties

Gregory E. Triplett[a]

Dept. of Electrical and Computer Engineering, Univ. of Missouri, Columbia, Missouri USA 65211

ABSTRACT

This study focuses on the influence of epi-layer strain and piezoelectric effects in asymmetric GaInAs/GaAlAs action regions that potentially lead to intra-cavity frequency mixing. The theoretical limits for conduction and valence band offsets in lattice-matched semiconductor structures have resulted in the deployment of non-traditional approaches such as strain compensation to extend wavelength in intersubband devices, where strain limits are related to misfit dislocation generation. Strain and piezoelectric effects have been studied and verified using select photonic device designs. Metrics under this effort also included dipole strength, oscillator strength, and offset of energy transitions, which are strongly correlated with induced piezoelectric effects. Unique photonic designs were simulated, modeled, and then fabricated using solid-source molecular beam epitaxy into photonic devices. The initial designs produce "lambda" wavelength, and the introduction of the piezoelectric effect resulted in "lambda/2" wavelength. More importantly, this work demonstrates that the theoretical cutoff wavelength in intersubband lasers can be overcome.

Keywords: quantum cascade lasers, molecular beam epitaxy, frequency mixing, strain, active region

1. INTRODUCTION

Historically, the development of optoelectronic devices, such as thermal detectors and lasers, has been especially instrumental particularly regarding the advancement of infrared applications and capabilities. Such technological improvements have revealed greater flexibility in bandstructure engineering and advanced photonic technologies for navigation and reconnaissance. Despite recent surges in laser technology, the development of state-of-the-art devices that operate in the <3.5μm region will stem from advancements in materials integration, device design, synthesis, as well as fabrication. Recent efforts to achieve 3-5 μm quantum cascade laser (QCL) devices have included wider-bandgap materials (i.e. nitrides) with large conduction band offsets (~2 eV), strain compensated QCLs, and harmonic generation processes; however, there is still much room for improvement. In this work, the ability to extend device operation within the 3-5 μm region is investigated through nonlinear processes *within* the cavity, with AlGaAs/(In)GaAs QCL structures as the test vehicle. The GaAs-based material system is appropriate for this study because it is technologically mature and it already has demonstrated the flexibility to achieve a uniquely wide range (7 to 100 μm) of wavelength.

There has been steadily growing interest in QCL devices, whose physical characteristics can be a few billionths of a meter. Since their demonstration in 1994 by Faist, et al. [1], these complex structures are the subject of intense research activity due to the quantum mechanical behavior of isolated charged particles (electrons) [2]. Through careful bandgap engineering of sequential semiconducting layers in a QCL device, an isolated charged particle can generate *numerous* photons with specific quantum properties. Until now, these unipolar devices have demonstrated photon emission across the mid-IR region of the electromagnetic spectrum making them useful for numerous IR applications that include remote sensing of chemical agents, detection of trace gases (CH_4 and N_2O), combustion diagnostics, LIDAR, and pollution monitoring. Despite the wide range of lasers previously available, QCLs have successfully filled some significant technological gaps. They are capable of kilohertz linewidth, providing lasing wavelengths far beyond the near IR region. Based on their design, most of the mid-IR spectrum can be covered by the same material. In comparison to other laser device designs, the key advantages of QCL devices are higher power and the *intersubband* transition that provides lasing at longer wavelengths, where narrow bandgap materials in interband devices are typically considered. For conventional laser diode structures, lasing wavelength is dependent on material bandgap and availability of both electron and hole states in the conduction and valence bands, respectively. Conversely, in QCL structures, only one *type* of particle is necessary and the wavelength of produced photons is not related to the bandgap of the semiconductor material.

Furthermore, each isolated electron in a QCL device can produce an individual photon at each stage in a series of sequential stages.

Over the past decade, the study of intersubband transitions in QCL devices have revealed numerous possibilities to produce photons that span the IR region of the electromagnetic spectrum, but this is limited to wavelengths above ~3.5 μm. Because QCL structures are unipolar, a large (~1 eV) conduction band offset (ΔE_c) could potentially extend operation well below 4 μm. For example, to achieve 1.55 μm (a typical free space optical communications wavelength), an 800 meV intersubband energy separation in a QCL structure is necessary, which includes II-VI materials [3], type-II heterostructures [4], and nitride materials [5]. However, experimental results have suggested that significant advancements in device simulations, growth, and fabrication are still necessary. One course of action includes the use of the nonlinear susceptibility. Nonlinear susceptibility can facilitate nonlinear polarization in a lasing medium, and as a result provide components with twice the frequency component, i.e. second-harmonic generation (SHG). In a report by Gmachl, et al. [6], devices demonstrated SHG in AlInAs/InGaAs QCLs with power levels up to 2 μW. Here, an AlInAs/InGaAs QCL laser designed for 7.5 μm light emission produced modes at 7.5 and 3.75 μm, respectively. In another report, Qu et al. [7] achieved a maximum linear-to-nonlinear power efficiency of 500μW/W^2 for AlInAs/InGaAs grown by molecular beam epitaxy on InP substrates. While important, these demonstrations only focused on InP-based systems and the second harmonic was more of a natural occurrence due to the large conduction band offset of lattice matched systems. Meanwhile, other materials technologies remain unexplored.

This technical approach involves molecular beamy epitaxy (MBE) growth of AlGaAs/(In)GaAs structures. The proposed test vehicles [8] are particularly appropriate for this study because AlGaAs is closely lattice matched to the GaAs substrate on which it is grown and various ΔE_c are not achievable without significant strain incorporation (i.e. the addition of indium). There exists, however, some design constraints. The AlGaAs alloy has a maximum Γ-point throughout the compositional range, and the aluminum composition must remain below 45%, otherwise the X-valley becomes lower than the Γ-point and QCL device performance quickly degrades. So, in order to get a larger conduction band offset, ΔE_c, at a fixed Al-concentration, indium is added to the GaAs quantum well region where the optical transition of the QCL takes place. In a strained $In_{0.04}Ga_{0.96}As$ well, for example, a 26 meV larger band offset compared to pure GaAs is obtained. Therefore, the use of AlGaAs/(In)GaAs strained quantum wells proposed will increase ΔE_c as well as the intersubband transitions [9-11].

At the same time, the InGaAs quantum well increases epi-layer strain between the AlGaAs layers. As a result, small critical layer thickness is expected along with modifications to conduction band properties. Fittingly, this work includes the use of (111) GaAs substrates for QCL growth, as this orientation strongly influences the strain relaxation mechanisms from the proposed laser design and allows for greater indium incorporation. Successful growth of QCLs on (111) is important for 3-5 μm emission in that it is a critical step in a series of steps for producing higher optical harmonic power [12].

2. QCL FUNDAMENTALS AND TECHNICAL CHALLENGES

The basis of a QCL structure is a *quantum well*, a three-layer structure where a smaller bandgap material is sandwiched between wider bandgap materials. This quantum well provides energetically favorable states (energy levels, E_n) for charged particles to reside. The flexibility in QCL design involves a mixture of various semiconductor materials through alloying and well and barrier thicknesses. There are several essential degrees of freedom to highlight. When the barriers (larger bandgap material) on each side of the quantum well are appropriately thick, the isolated charged particles are confined to the quantum well. When barriers are thinner, the charged particles can tunnel through the *thin* barrier into the adjacent quantum well. When the quantum well (lower bandgap material) is appropriately thick, the charge particles reside in lower energy states in the conduction band. When the quantum well is *thinner*, the ground state is "squeezed" upwards as a result of quantization and the charged carriers exhibit specific energetic properties. QCLs utilize a cascading active core (sequences of quantum wells/barriers) so that electrons essentially travel (through control of tunneling) downstream emitting photons at the steps of the cascading layer.

QCL emission is based on intersubband transitions involving electrons and electron energy levels, E_n, where n is 1, 2, 3, etc. The intersubbands, E_n, in these structures are controlled by the applied bias (V_a) and properties of the quantum wells and barriers. The quantum wells and barriers in QCLs are thin for the purpose of coupling the electron wavefunctions, which is essential for the lasing medium. As the electrons leave the injector region and tunnel into the active medium, they reside in the quantum well at the high energy level (E_3). After some time, τ_3, electrons fall to a lower available energy state, E_2, and emit photons with energy, E_{ph}, correlating with the change (ΔE) in energy states

(i.e. $E_3 \rightarrow E_2 = \Delta E$). As is the case for conventional lasers, the necessary condition for lasing in QCLs is population inversion—$N_3 > N_2$, where N_3 is the population at E_3 and N_2 is the population at E_2.

In order for population inversion to be maintained in these structures, the lower level, E_2, needs fast depopulation of electrons to the ground state or E_1 level. Taking into account resonant longitudinal-optical (LO)-phonon scattering times that are very short, (<1 picosecond), the $E_2 \rightarrow E_1$ transition is appropriately designed for the LO-phonon energy (~30 meV). Ironically, this LO phonon energy makes it challenging for AlGaAs/GaAs QCLs to emit in the THz range at room temperature. As E_{32} transition lifetime remains longer than E_2 carrier lifetime ($\tau_{32} > \tau_2$), population inversion is obtained. Typically, τ_{32} is on the order of several picoseconds. With appropriate selection of the scattering rates, only E_3 and the ground state have significant electron population. Evaluation of a QCL design using the gain coefficient, g, can be calculated as follows [13]:

$$ g \ \alpha \ \tau_3 \left(1 - \frac{\tau_2}{\tau_{32}}\right) \frac{4\pi e z_{32}^2}{\lambda_1 \mu_{eff} L_p} \frac{1}{\gamma_{32}} \qquad (1) $$

where τ_3 is the LO-phonon scattering time between E_3 and E_2, e is the electron charge, λ_1 is the laser wavelength, μ_{eff} is the modal effective refractive index at λ_1, L_p is the thickness of one pair of active region and injection, z_{32} is the optical dipole matrix element, and γ_{32} is the full-width-half-maximum (FHWM) of the E_{32} transition. As apparent from Equation 1, gain can be enhanced when the E_{32} transition time is long and the dipole matrix element is large.

Because alignment of injector subbands and upper radiation levels in the active region is necessary, changes in thickness over a few monolayers stemming from strain effects can have significant effects on subband energy separations, which are already small for wavelengths in the mid-IR region. Strain control remains a challenge for broad implementation and high-volume production of QCLs. For example, the emission spectrum for a well-designed QCL is so narrow that broadening of intersubband transitions due to strain effects is associated with a FHWM of 10-20 meV in the mid-IR range [14]. Since the proposed structures are based on AlGaAs/(In)GaAs material systems, where the strain increases with indium composition, the lattice mismatch (f) between InAs and (Al)GaAs must be carefully managed. These and other factors make it particularly challenging (and interesting as well) to synthesize AlGaAs/(In)GaAs QCL structures. Fittingly, the experimental methods for synthesizing these structures is MBE, a technology that provides strict atomic layer control for multi-layer structures. MBE allows strain monitoring of InAs-based quantum wells [15, 16].

Overall, the design of a QCL structure can be very involved. A typical QCL structure can include up to one-thousand individual layers that have dimensions on the order of several nanometers. QCL devices can be re-produced only when strict control of layer thickness is available and strain effects are minimized. This is one of the primary reasons that AlGaAs/GaAs and InAlAs/InGaAs/InP lattice-matched systems have gained so much attention. Still in its developmental stages, QCLs have neither been optimized nor implemented using a wide selection of semiconductor material systems. The ability to improve and expand the performance capabilities of QCLs is strongly related to the controlled integration of numerous materials and various designs. Moreover, there are additional technical challenges that include QCL wall-plug efficiency [17], high-frequency (~100 GHz) modulation [18], and cost. For these reasons, the exploration of strained AlGaAs/(In)GaAs QCL structures is significant and has a broader impact, i.e. it brings new knowledge to the QCL field. The next section describes the technical issues with achieving high power 3-5 µm emission in QCLs.

3. NON-LINEAR OPTICAL PHENOMENA IN QCLS

The ability to produce 3-5 µm emission in QCLs is complicated, as previously described. A considerable amount of attention has been directed towards the use of nonlinear processes in other optical devices; however, non-linear optical phenomena have been relatively unexplored in QCL structures. If nonlinear optical processes are integrated *within* the laser cavity, the development of high-power QCLs that operate in the 3-5 µm range is certainly foreseeable. One of the major technical challenges has been the linear-to-nonlinear power conversion efficiency, which is strongly related to nonlinear susceptibility and phase matching of the fundamental and nonlinear light. A promising solution for maximum power conversion and phase matching is a monolithic and guided wave approach [6]. In this approach, the laser radiation generated by the intersubband transitions would act as an intracavity optical pump for nonlinear wavelength conversion. There are several basic approaches to integrating optical nonlinearity within a QCL that include designed quantum wells in the waveguide core and multi-purpose use of the active region in the QCL for nonlinear wavelength conversion. Several reports have shown that each approach has its advantages and that the real drawback remains the phase matching

of the waveguides. Instead, much attention has been placed on optimization of the nonlinear susceptibility, $\chi^{(2)}$, which can be approximated as follows [19]:

$$\chi^{(2)} \; \alpha \; e^3 \; N_e \frac{z_{i-ii}z_{ii-iii}z_{i-iii}}{\left(\hbar\omega - E_{i-ii} - i \cdot \gamma_{i-ii}\right) \cdot \left(2\hbar\omega - E_{i-iii} - i \cdot \gamma_{i-iii}\right)} \tag{2}$$

where N_e is the electron density in the active region, E_{j-k} and $2\gamma_{j-k}$ are the energy difference and transition broadenings between energy levels j and k when $j, k = i, ii, iii$. Here, an optimized linear conversion process requires that one of the energy levels (i, ii, iii) be sufficiently populated with electrons. Since the upper level, E_3, is sufficiently populated in the active region, a feasible design for nonlinear wavelength conversion will include overlapping E_3 with one level in the nonlinear region.

In a study by Gmachl, et al [6], harmonic generation was explored using AlInAs/InGaAs structures grown by MBE on InP that emitted fundamental modes at 9.1 µm and 7.5 µm and SHG light at 4.55 µm and 3.75 µm, respectively. This group explored optical nonlinearity that was integrated into the laser active regions and achieved SHG power levels up to 2µW with a linear-to-nonlinear power conversion efficiency of 50-100 µW/W^2. These values are not extremely high, but the demonstration holds promise as phase matching between the fundamental and SHG was lacking.

In a later study by Malis, et al [20], similar structures were examined with a phase matching approach and at least a two-order magnitude improvement in SHG and nonlinear power conversion efficiency was demonstrated. Phase matching was accomplished using an appropriate decrease of the modal refractive index of the fundamental light relative to the modal refractive index of the SHG light. This was achieved through the dependence of the effective refractive index on the ridge width.

In another study by Qu, et al. [7], the nonlinear power conversion efficiency was explored using AlInAs/InGaAs structures grown by MBE on InP without modal phase matching. They found the nonlinear power conversion to also be strongly dependent on the injection current density due to an electric field and current dependent nonlinear susceptibility. The nonlinear power conversion efficiency was shown to increase by one order of magnitude over the current density range (2.7 - 7.5 kA/cm^2) and electric field range (43.5 - 57 kV/cm) to provide maximum efficiency of 500 µW/W^2. These results show particular promise for tuning the nonlinearity based on current density and applied bias.

Austerer, et al. [21] also studied SHG in QCLs, but employed GaAs-based material systems. The $Al_{0.45}Ga_{0.55}As$/GaAs QCL structures were designed for 8-10 µm emission and phase matching was explored using symmetric double-plasmon waveguide based on low-doped GaAs core region and highly doped GaAs cladding region as well as a double AlGaAs waveguide. In the case of the doped GaAs core and cladding, the confinement for the second harmonic was not optimum. Improvements in modal confinement, however, were observed for double AlGaAs waveguide and the nonlinear power conversion efficiency was 100 µW/W^2 with nonlinear peak powers exceeding 100 µW. As in the study by Malis, et al [20], the power conversion efficiency was also dependent on ridge width.

The studies referenced herein imply that it is feasible to produce second harmonics in QCL structures. However, the challenges include optimum phase matching, modal confinement, and nonlinear susceptibility optimization.

4. QCL GROWTH ON (111) SUBSTRATES

QCLs are routinely produced on (100) GaAs and InP substrates. Given that the growth of QCLs is already complex, growth on (111) surfaces and various offsets would involve additional strain and piezoelectric effects that must be considered in the initial device design. Growth on (100) surfaces leaves the shape of the quantum wells in injector and active regions relatively unchanged by carrier injection. On the other hand, QCL growth on (111) surfaces brings into effect strain and piezoelectric influence and provides an additional degree of freedom for QCL device designers. Specifically, the piezoelectric effect in AlGaAs/(In)GaAs QCL structures introduces piezoelectric charges at the QW heterojunction and built-in electric fields in the QW. The promise of QCL devices grown on (111) surfaces lies in a tunable laser with a greater tuning range in which the gain peak of the laser cavity is manipulated [22].

The piezoelectric effect stemming from strained superlattice growth on (111) substrates is not a novel concept [23]. There have been numerous studies on this topic as well as the actual magnitude of the piezoelectric field in bulk layers, quantum wells [24-26], and more recently quantum dots [27, 28]. However, interest in the optical properties of films grown on (111) surfaces has been increasing. Implementation of the piezoelectric effect in QCLs leads to interesting flexibilities in QCL production, perhaps QCLs for telecommunications applications and applications where laser device tunability is a criterion.

Laser device growth on (111) surfaces has been previously demonstrated and there are notable advantages [22, 29-32]. Khoo, et al [22] examined *single* quantum well AlGaAs/InGaAs lasers grown on (111) GaAs substrates and

measured low threshold current density as low as 87 A/cm^2. In another study by Deligeorgis, et al [30], AlGaAs/InGaAs *laser diodes* on (111) GaAs substrates were found to also have reduced threshold current compared to (100) devices. The sources of reduced threshold current were attributed to reduced density of states (especially in heavy-hole states) and spontaneous emission rate. Likewise, QCL device growth on (111) substrates has also been explored. In a study by Giovannini, et al. [31], AlInAs/InGaAs QCL devices on InP were designed to emit at 6 μm and 10 μm. Unlike laser diodes, reduced threshold currents were not observed. In fact, the threshold current was twice as large as the same structure on (100) substrates. The sources of increased threshold current were attributed to one-order of magnitude higher doping in the (111) substrate and the growth quality of the structures. Still, second harmonics were observed, although the devices need further optimization regarding *phase matching* and performance at the fundamental mode.

The growth of QCLs on (100) substrates has been carefully studied, whereas the flexibility offered by (111) substrates remains somewhat unexplored. Actually, MBE growth on (111) substrates requires special operating conditions. The growth conditions are unlike those for (100) surfaces and the growth window for (111) substrates is much narrower [33]. In essence, the material quality on (111) surfaces is very sensitive to the growth conditions. Several groups have explored the growth conditions for arsenic-based material and found that good structural and electrical characteristics require lower arsenic overpressure along with higher growth temperature, which depends on the misorientation angle of the (111) substrate [34, 35]. These conditions are contrary to the conditions necessary for growth on (100) surfaces. The development of process models that describe strained layer growth on (111) substrates would aid in this regard.

Cho, et al. [36] studied interfacial properties of strained piezoelectric InGaAs structures on (111) GaAs substrates. Results show that not only are atomically smoother interfaces possible for highly strained wells, but also the LO phonon energy (~37 meV) is comparable with strained InGaAs wells grown on (100) surfaces. In another study by Marcadet, et al. [34], GaAs step flow growth on (111) GaAs by MBE was examined. In order to obtain mirror-like surfaces, the governing MBE growth parameters were substrate temperature and As:Ga ratio. Results show that surface morphology was driven by substrate misorientation angle, where lower misorientation (0.5°) has a higher growth temperature limit, and higher misorientation (2°) has a lower growth temperature limit. Clearly, the substrate temperature influences the probability for Ga adatoms to reach the step edges that facilitate step flow growth. That is, for samples tilted towards the $[2\,\bar{1}\,\bar{1}]$, step flow growth mode is required for smooth films.

Substrate growth temperature controls the Ga adatoms surface diffusion length and is responsible for *smooth* films. With control of Ga adatoms surface diffusion length and understanding that the growth kinetics are comparable for other III-V arsenic-based material, excellent material quality for the AlGaAs/(In)GaAs QCL structures is obtainable [29]. Similar MBE growth conditions are employed for simulated AlGaAs/(In)GaAs QCL structures on (111) GaAs [37].

5. TECHNICAL APPROACH TO PRODUCING 3-5μM QCLS

Like other groups that introduce strain-balancing strategies in QCL designs [38], this work targets a shorter wavelength QCL design space using nonlinear structures. One active region and one injector region is shown with a bias of 42 kV/cm, and the indium composition in the InGaAs quantum well was simulated at 4%. The wavefunctions E_1, E_2, E_3, and E_4 highlight important laser transition states in this structure where photons are produced through E_4-E_2 transitions and LO phonons through E_2-E_1 transitions. The structure from left to right (with values in nanometers, n-doped underlined and active region in bold) is the following: 2.8, 3.4, 1.7, 3.0, 1.8, 2.8, 2.0, 3.0, 2.6, 3.0, 4.6, **1.9**, 1.1, **5.4**, 1.1, **4.8**, 2.8, 3.4, 1.7, 3.0, 1.8, 2.0, 3.0, 2.6, 3.0. The use of indium in the GaAs quantum well increases ΔE_c (~33meV for unstrained; 26meV for strained [39]) without increasing the aluminum composition to an indirect semiconductor material where electrons scatter more efficiently into the X-valley. According to the Matthews and Blakeslee model [40, 41], strained InGaAs layers can be synthesized up to at least 10-nm with 25% indium composition. Therefore, the range is rather wide.
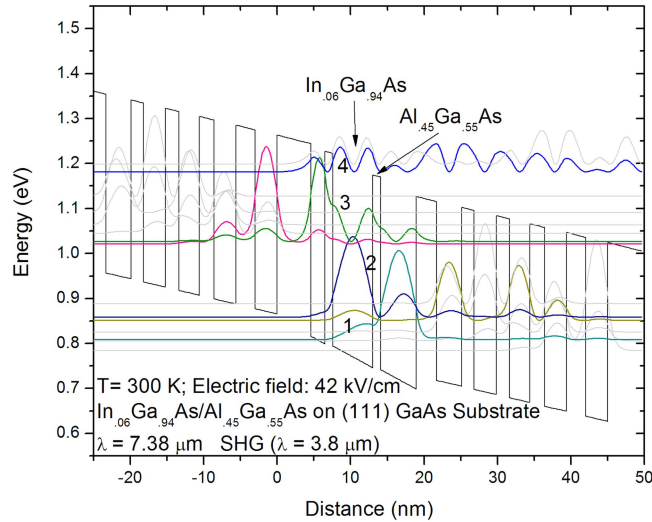
Figure 1. (a) Simulation of AlGaAs/(In)GaAs starting QCL structure on (111) with a bias of 42 kV/cm.

Device tunability is an especially important performance criterion for these devices. Data in Figure 2 shows the influence that electric field has on the oscillator strength between states E_{3-2} (the first harmonic). The oscillator strength shows a general trend that *increases* with applied electric field, which also *increases* intersubband separation. Here, the electric field values for all structures with 1% to 6% indium in the active region were varied from 38kV/cm up to 55kV/cm. By optimizing the oscillator strength and realizing electric field tunability, this work enables natural nonlinear processes within the cavity. For example, by comparing oscillator strength data and electric field tunability with the optimum nonlinear susceptibility data, these design spaces are found to overlap, which suggests that propagation of higher order harmonic generation is likely in GaAs-based QC lasers. Figure 3 illustrates nonlinear susceptibility values extracted from selectively strained quantum well layers in the active region. It is apparent that the nonlinear susceptibility is both tunable with applied electric field and sensitive to compressive strain. Even though the second harmonic optical power is low in traditional QCL structures, these results suggest that GaAs based devices can successfully carry higher order harmonics produced.
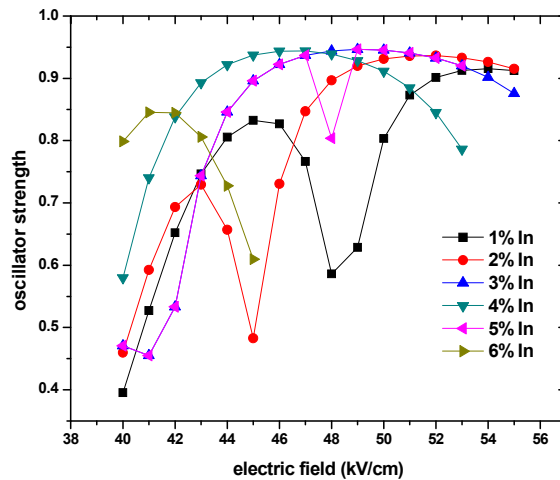

Figure 2. Oscillator strength of the 3 to 2 transition for InGaAs/AlGaAs active well region.
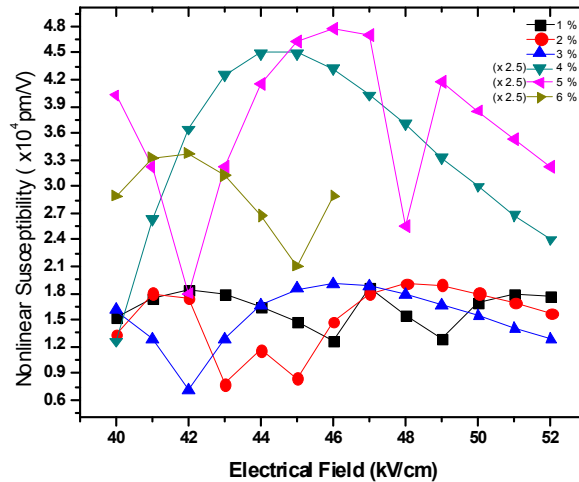
Figure 3. Nonlinear susceptibility values for selectively strained InGaAs-based QC laser.

Because four wavefunctions essentially determine the functionality of these laser structures, measuring wavefunction separations is necessary. Spectroscopic analysis was performed to measure these separations [42], and 7 micron (E_4-E_3 normal laser transition), and 3.8 micron (E_4-E_2 transition - due to the frequency mixing) associated with the laser design were observed. Experimental data reveals all of the peaks mentioned above including the impact of misoriented (111) vs (100) orientation, thus showing the piezoelectric effect has been effectively incorporated.

6. CONCLUSION

This work explores the shifting of the beam wavelength limit in quantum cascade lasers (QCLs) through the implementation of the piezoelectric effect. By doing so, unique intracavity characteristics produced both fundamental and higher order modes. In this demonstration, the QCL design that was fabricated included AlGaAs/InGaAs active and injector regions on a [111] GaAs matrix, where strain was incorporated in an asymmetric three-quantum well active region and a fourth intersubband was introduced without compromising crystal quality.

ACKNOWLEDEGEMENTS

REFERENCES

1.   Faist, J., Capasso, F., Sivco, D.L., Sirtori, C., Hutchinson, A.L., and Cho, A.Y., *Quantum cascade laser.* Science, 1994. **264**(5158): p. 553-6.
2.   Gmachl, C., Capasso, F., Sivco, D.L., and Cho, A.Y., *Recent progress in quantum cascade lasers and applications.* Reports on Progress in Physics, 2001. **64**(11): p. 1533-601.
3.   Akimoto, R., Kinpara, Y., Akita, K., Sasaki, F., and Kobayashi, S., *Short-wavelength intersubband transitions down to 1.6 mum in ZnSe/BeTe type-II superlattices.* Applied Physics Letters, 2001. **78**(5): p. 580-2.
4.   Ohtani, K. and Ohno, H., *Intersubband electroluminescence in InAs/GaSb/AlSb type-II cascade structures.* Applied Physics Letters, 1999. **74**(10): p. 1409-11.
5.   Nevou, L., Tchernycheva, M., Julien, F.H., Guillot, F., and Monroy, E., *Short wavelength (lambda=2.13 mum) intersubband luminescence from GaN/AlN quantum wells at room temperature.* Applied Physics Letters, 2007. **90**(12): p. 121106-1-3.

6. Gmachl, C., Belyanin, A., Sivco, D.L., Peabody, M.L., Owschimikow, N., Sergent, A.M., Capasso, F., and Cho, A.Y., *Optimized second-harmonic generation in quantum cascade lasers.* IEEE Journal of Quantum Electronics, 2003. **39**(11): p. 1345-55.

7. Qu, D., Feng, X., Shu, G., Momen, S., Narimanov, E., Gmachl, C.F., and Sivco, D.L., *Second-harmonic generation in quantum cascade lasers with electric field and current dependent nonlinear susceptibility.* Applied Physics Letters, 2007. **90**(3): p. 31105-1-3.

8. Sirtori, C., Kruck, P., Barbieri, S., Collot, P., Nagle, J., Beck, M., Faist, J., and Oesterle, U., *GaAs/Al_xGa_{1-x}As quantum cascade lasers.* Applied Physics Letters, 1998. **73**(24): p. 3486-8.

9. Chui, H.C., Martinet, E.L., Fejer, M.M., and Harris, J.S., Jr., *Short wavelength intersubband transitions in InGaAs/AlGaAs quantum wells grown on GaAs.* Applied Physics Letters, 1994. **64**(6): p. 736-8.

10. Jancu, J.M., Pellegrini, V., Colombelli, R., Beltram, F., Mueller, B., Sorba, L., and Franciosi, A., *Quantum tailoring of optical transitions in In_xGa_{1-x}As/AlAs strained quantum wells.* Applied Physics Letters, 1998. **73**(18): p. 2621-3.

11. Asano, T., Noda, S., Abe, T., and Sasaki, A., *Investigation of short wavelength intersubband transitions in InGaAs/AlAs quantum wells on GaAs substrate.* Journal of Applied Physics, 1997. **82**(7): p. 3385-91.

12. Bliss, D.F., Lynch, C., Weyburne, D., O'Hearn, K., and Bailey, J.S., *Epitaxial growth of thick GaAs on orientation-patterned wafers for nonlinear optical applications.* Journal of Crystal Growth, 2006. **287**(2): p. 673-678.

13. Faist, J., Capasso, F., Sirtori, C., Sivco, D.L., Baillargeon, J.N., Hutchinson, A.L., Chu, S.N., and Cho, A.Y., *High power mid-infrared (lambda~5 mum) quantum cascade lasers operating above room temperature.* Applied Physics Letters, 1996. **68**(26): p. 3680-2.

14. Faist, J., Capasso, F., Sirtori, C., Sivco, D.L., Hutchinson, A.L., Chu, S.N.G., and Cho, A.Y., *Narrowing of the intersubband electroluminescent spectrum in coupled-quantum-well heterostructures.* Applied Physics Letters, 1994. **65**(1): p. 94-6.

15. Triplett, G.E., Brown, A.S., and May, G.S., *Interrelationships in the electronic and structural characteristics of strained InAs quantum well structures.* Journal of Crystal Growth, 2006. **286**(2): p. 345-349.

16. Triplett, G.E., Brown, A.S., and May, G.S., *Strain monitoring in InAs-Al_xGa_{1-x}As_ySb_{1-y} structures grown by molecular beam epitaxy.* Applied Physics Letters, 2006. **89**(3): p. 32106-1-3.

17. Vurgaftman, I. and Meyer, J.R., *Analysis of limitations to wallplug efficiency and output power for quantum cascade lasers.* Journal of Applied Physics, 2006. **99**(12): p. 123108-1-7.

18. Vurgaftman, I., Yeeloy, L., and Singh, J., *Carrier thermalization in sub-three-dimensional electronic systems: fundamental limits on modulation bandwidth in semiconductor lasers.* Physical Review B (Condensed Matter), 1994. **50**(19): p. 14309-26.

19. Capasso, F., Sirtori, C., and Cho, A.Y., *Coupled quantum well semiconductors with giant electric field tunable nonlinear optical properties in the infrared.* IEEE Journal of Quantum Electronics, 1994. **30**(5): p. 1313-26.

20. Malis, O., Belyanin, A., Gmachl, C., Sivco, D.L., Peabody, M.L., Sergent, A.M., and Cho, A.Y., *Improvement of second-harmonic generation in quantum-cascade lasers with true phase matching.* Applied Physics Letters, 2004. **84**(15): p. 2721-3.

21. Austerer, M., Schartner, S., Pflugl, C., Andrews, A.M., Roch, T., Schrenk, W., and Strasser, G., *Second-harmonic generation in GaAs-based quantum-cascade lasers.* Physica E, 2006. **35**(2): p. 234-40.

22. Khoo, E.A., Pabla, A.S., Woodhead, J., David, J.P.R., Grey, R., and Rees, G.J., *Low threshold InGaAs/AlGaAs lasers grown on (111)B GaAs substrate.* Electronics Letters, 1997. **33**(11): p. 957-8.

23. Mailhiot, C. and Smith, D.L., *Electromodulation of the electronic structure and optical properties of [111]-growth-axis superlattices.* Physical Review B (Condensed Matter), 1988. **37**(17): p. 10415-18.

24. Goossen, K.W., Caridi, E.A., Chang, T.Y., Stark, J.B., Miller, D.A.B., and Morgan, R.A., *Observation of room-temperature blue shift and bistability in a strained InGaAs-GaAs <111> self-electro-optic effect device.* Applied Physics Letters, 1990. **56**(8): p. 715-17.

25. Bahder, T.B., *Converse piezoelectric effect in [111] strained-layer heterostructures.* Physical Review B (Condensed Matter), 1995. **51**(16): p. 10892-6.

26. Moise, T.S., Guido, L.J., and Barker, R.C., *Magnitude of the piezoelectric field in (111)B In_yGa_{1-y}As strained-layer quantum wells.* Journal of Applied Physics, 1993. **74**(7): p. 4681-4.

27.   Bester, G. and Zunger, A., *Cylindrically shaped zinc-blende semiconductor quantum dots do not have cylindrical symmetry: atomistic symmetry, atomic relaxation, and piezoelectric effects.* Physical Review B (Condensed Matter and Materials Physics), 2005. **71**(4): p. 45318-1-12.

28.   Ranjan, V., Allan, G., Priester, C., and Delerue, C., *Self-consistent calculations of the optical properties of GaN quantum dots.* Physical Review B (Condensed Matter and Materials Physics), 2003. **68**(11): p. 115305-1-7.

29.   Marcadet, X., Ortiz, V., Bengloan, J.Y., Dhillon, S., Calligaro, M., and Sirtori, C., *Molecular-beam epitaxy growth of quantum cascade lasers on (111)B substrates for second harmonic generation.* Journal of Vacuum Science & Technology B (Microelectronics and Nanometer Structures), 2004. **22**(3): p. 1558-61.

30.   Deligeorgis, G., Dialynas, G.E., Hatzopoulos, Z., and Pelekanos, N.T., *Threshold current reduction due to piezoelectric effects in InGaAs/AlGaAs laser diodes.* Journal of Physics: Conference Series, 2005. **10**(1): p. 35-8.

31.   Giovannini, M., Beck, M., Hoyler, N., and Faist, J., *Second harmonic generation in (111)-oriented InP-based quantum cascade laser.* Journal of Applied Physics, 2007. **101**(10): p. 103107-1-4.

32.   Dialynas, G.E., Deligeorgis, G., Le Thomas, N., Hatzopoulos, Z., and Pelekanos, N.T. *Comparative study of (100) and (111)B InGaAs single quantum well laser diodes.* in *Fifth International Workshop on Epitaxial Semiconductors on Patterned Substrates and Novel Index Surfaces (ESPS-NIS). Stuttgart, Germany. 13-15 Oct. 2003.* 2004.

33.   Yeo, W., Dimitrov, R., Schaff, W.J., and Eastman, L.F., *The effect of As$_4$ pressure on material qualities of AlGaAs/GaAs heterostructures grown on (111)B GaAs substrates.* Applied Physics Letters, 2000. **77**(17): p. 2764-6.

34.   Marcadet, X., Olivier, J., and Nagle, J. *Stability of the step distribution and MBE growth mechanisms on vicinal GaAs (111) substrates.* in *Sixth International Conference on the Formation of Semiconductor Interfaces. Cardiff, UK. British Assoc. Crystal Growth. British Tourist Authority. IOP. et al. 23-27 June 1997.* 1998.

35.   Hayakawa, T., Morishima, M., and Chen, S., *Surface reconstruction limited mechanism of molecular-beam epitaxial growth of AlGaAs on (111)B face.* Applied Physics Letters, 1991. **59**(25): p. 3321-3.

36.   Cho, Soohaeng; Sanz-Hervás, A.; Kim, Jongseok; Majerfeld, A.; Kim, B. W. *Interfacial properties of strained piezoelectric InGaAs/GaAs quantum wells grown by metalorganic vapor phase epitaxy on (111)A GaAs.* Journal of Applied Physics, 2004. **96**(4): p. 1909-13.

37.   Triplett, G., Roberts, D., and Ikpe, S. *Enhancing oscillator strength for second harmonic generation in AlGaAs/InGaAs quantum cascade laser structures.* in *IEEE Laser and Electro-Optics Society (LEOS) Conference.* 2009. Newport Beach, CA.

38.   Evans,   A.   and   Razeghi,   M.,   *Reliability   of   strain-balanced Ga$_{0.331}$In$_{0.669}$As/Al$_{0.659}$In$_{0.341}$As/InP quantum-cascade lasers under continuous-wave room-temperature operation.* Applied Physics Letters, 2006. **88**(26): p. 261106-1-3.

39.   Gianordoli, S., Schrenk, W., Hvozdara, L., Finger, N., Strasser, G., and Gornik, E., *Strained InGaAs/AlGaAs/GaAs-quantum cascade lasers.* Applied Physics Letters, 2000. **76**(23): p. 3361-3.

40.   Coleman, J.J., *Strained-layer InGaAs quantum-well heterostructure lasers.* IEEE Journal of Selected Topics in Quantum Electronics, 2000. **6**(6): p. 1008-13.

41.   Matthews, J.W. and Blakeslee, A.E., *Defects in epitaxial multilayers. I. Misfit dislocations.* Journal of Crystal Growth, 1974. **27**(1): p. 118-25.

42.   Meyer, C., Cheng, E., Grayer, J., Mueller, D., Triplett, G., Roberts, D., and Graham, S., "Pseudomorphic growth of InAs on misoriented GaAs for extending quantum cascade laser wavelength", Journal of Vacuum Science & Technology A, 31, 06F109 (2013)